

**SYNTHESIS AND CHARACTERIZATION OF
POLYANILINE/MULTIWALLED CARBON NANOTUBES BASED
NANOCOMPOSITES**

by

SAIFUL IZWAN ABD RAZAK

**Thesis submitted in fulfillment of the requirements
for the degree of
Master of Science**

October 2010

ACKNOWLEDGEMENT

In the name of Allah the most beneficent and the most merciful, all praise and thanks are due to Allah the creator and sustainer of the worlds and His Messenger Muhammad S.A.W for his bonds of love.

I would like to address my deepest wholehearted gratitude to my supervisor, Associate Prof. Dr. Sharif Hussein Sharif Zein, for his continuing support and mentorship in completing this project within limited time frame. I would like to thank him for his enthusiasm and understanding that was shown throughout the period. The appreciation also goes to my co-supervisor, Prof. Dr. Abdul Latif Ahmad for providing me the valuable chance to do my study and research here in Universiti Sains Malaysia. I would also like to thank Prof. Aldo Boccaccini for his valuable discussion regarding the project.

My special appreciation goes to all my lecturers during my undergraduate study in the Department of Materials Science, Asian Institute of Medicine Science and Technology for giving me a strong knowledge foundation that have helped me substantially during my research.

Finally, I would like to take this opportunity to thank my parents, Dato' Abd. Razak Hassan and Datin Khalizah Kahar, whose love, support, eternal dedication and devotion which had shaped and inspired my life. My appreciation also goes to Noor Fadzlina who had always stick with me through hardship and joy.

TABLE OF CONTENTS

	Page
Acknowledgements	ii
Table of Contents	iii
List of Tables	vii
List of Figures	viii
List of Plates	xiii
List of Abbreviations	xiv
List of Symbols	xv
Abstrak	xvi
Abstract	xviii

CHAPTER 1: INTRODUCTION

1.1 Overview	1
1.2 Problem Statement	4
1.3 Research Objectives	6
1.4 Scope of study	6

CHAPTER 2: LITERATURE REVIEW

2.1 Nanotechnology	8
2.1.1 Nanomaterials	11
2.1.2 Properties and application carbon nanotubes (CNTs)	

and other allotropes of carbon	13
2.1.3 Functionalization of carbon nanotubes (CNTs)	26
2.2 Composite materials	32
2.2.1 Definition	32
2.2.2 Classification of dispersed phase	34
2.2.3 Polymer matrix composite	37
2.2.4 Nanocomposite	39
2.2.5 Interaction between matrix and reinforcement	40
2.3 Conducting polymers	42
2.3.1 Applications of conducting polymers	43
2.3.2 Polyacetylene	47
2.3.3 Poly(ethylenedioxythiophene) (PEDOT)	48
2.3.4 Polypyrrole (PPy)	49
2.3.5 Polyaniline (PANI)	50
2.3.5.1 Synthesis and properties of polyaniline (PANI)	53
2.3.5.2 PANI/MWCNTs nanocomposites	56
2.3.5.3 PANI based nanocomposites with other types of nonconducting reinforcement	64
2.3.6 Percolation threshold	66
2.3.7 Conductivity of materials and conducting polymers	68
2.4 Manganese	70
2.5 Principle of instrumentation	71

CHAPTER 3: MATERIALS AND METHODS

3.1 Materials and reagents	74
3.2 Experimental method	75
3.2.1 Filling of MnO ₂ in MWCNTs	75
3.2.2 Polymerization of neat PANI	76
3.2.3 Deprotonation of neat PANI	77
3.2.4 Ex-situ preparation of ES-PANI/MWCNTs-MnO ₂ nanocomposite	77
3.2.5 In-situ preparation of ES-PANI/MWCNTs-MnO ₂ nanocomposite	78
3.2.6 Deprotonation of ES-PANI/MWCNTs-MnO ₂ nanocomposite	79
3.3 Characterization and testing	80
3.3.1 Interaction and structural characterization	80
3.3.2 Thermal characterization	80
3.3.3 Electron microscopy	81
3.3.4 ES nanocomposites with different MWCNTs-MnO ₂ loading	81
3.3.5 Conductivity ageing testing	81
3.3.6 Percolation threshold	81
3.3.7 Reprotonation testing	82
3.3.8 Solubility, colour characteristic and film formation	82
3.3.9 Conductivity measurement and calculation	83
3.4 Schematic diagram of research methodology	85

CHAPTER 4: RESULTS AND DISCUSSION

4.1 Effect of MnO ₂ filling on the properties of MWCNTs	86
4.2 Effect of potassium dichromate, K-feldspar and ammonium persulfate as oxidizing agents on the properties of polymerized PANI	92
4.3 Properties of ex situ prepared ES-PANI/MWCNTs-MnO ₂ nanocomposites and effect of PHBSA	102
4.4 Properties of in situ prepared ES-PANI/MWCNTs-MnO ₂ nanocomposites	108
4.5 Effect of MWCNTs-MnO ₂ loading on the properties of in-situ prepared ES-PANI/MWCNTs-MnO ₂ nanocomposites, its non conducting electrical percolation threshold, doping reversibility and conductivity ageing	126
4.6 Solubility, colour characteristic and film formation of in-situ prepared ES-PANI/MWCNTs-MnO ₂ nanocomposites	144

CHAPTER 5: CONCLUSIONS

5.1 Conclusions	149
5.2 Suggestions for further study	153

REFERENCES	155
-------------------	-----

LIST OF PUBLICATIONS AND CONFRENCES	189
--	-----

LIST OF TABLES

		Page
2.1	PANI/MWCNTs and its conductivity or resistivity.	58
4.1	Yield of PANI at different MWCNTs/MnO ₂ loading	128
4.2	Calculated and experimental conductivity values of the dedoped PANI/MWCNTs-MnO ₂ nanocomposites at different loading	141
4.3	Conductivity of nanocomposites after 1 week, 2 weeks and 4 weeks	144

LIST OF FIGURES

	Page
2.1 Physical structure of graphite	14
2.2 Physical structure of diamond	15
2.3 Physical structure of fullerene	17
2.4 Physical structure of SWCNT	18
2.5 Rolling up graphene sheet to form zigzag, armchair and chiral SWCNT	19
2.6 Physical structure of MWCNT	20
2.7 Molecular dynamics simulation of a) single kink of bending b) under torsion of a SWCNT	22
2.8 Sketch of the CNT array on a silicon wafer	23
2.9 A single MWCNT interconnect	25
2.10 Transparent thin-film transistors of CNTs	25
2.11 Typical defects in SWCNT	28
2.12 Octadecylamine functionalization of SWCNTs	29
2.13 Chemical modification of CNTs through oxidation followed by the esterification or amidization of the carboxyl groups	30
2.14 Wrapping of polystyrene on MWCNTs	31
2.15 Wrapping of peptide on SWCNTs	31
2.16 Wrapping of dodecyltrimethylammonium bromide on SWCNTs and deoxyribonucleic acid	31
2.17 Classification of composite materials	35
2.18 Possible interactions between matrix and reinforcement a) mechanical interlocking. b) electrostatic c) coupling agent	42

2.19	Conductivity of conducting polymers compared other materials	43
2.20	Schematic of a biosensor	44
2.21	Cross section of conducting polymer light emitting diode	46
2.22	A flexible, semitransparent plastic chip using conducting PANI	46
2.23	The chain structure of a) <i>cis</i> -polyacetylene and b) <i>trans</i> -polyacetylene	48
2.24	Repeating unit of poly(ethylenedioxythiophene)	49
2.25	Repeating unit of polypyrrole	50
2.26	The different oxidation states in PANI: a) leucoemeraldine b) emeraldine c) nigraniline d) pernigraniline	52
2.27	Reversible transformations from ES to EB of PANI	53
2.28	Reaction mechanism of polyaniline via radical cation polymerization	54
2.29	Schematic representation of Fe ₃ O ₄ /PANI/MWCNTs	64
3.1	Schematic diagram of the a) oxidation b) MnO ₂ filling and c) carboxylation of MWCNTs	75
3.2	Schematic diagram of the polymerization process of neat PANI	76
3.3	Schematic of the deprotonation of neat PANI	77
3.4	Schematic preparations of ex-situ ES-PANI/MWCNTs-MnO ₂ nanocomposites	78
3.5	Schematic preparations of PHBSA doped ex-situ ES-PANI/MWCNTs-MnO ₂ nanocomposites	78
3.6	Schematic preparations of in-situ ES-PANI/MWCNTs-MnO ₂ nanocomposites	79
3.7	Schematic of the deprotonation of in-situ PANI/MWCNTs-MnO ₂ nanocomposites	80
3.8	Schematic diagram of the research methodology	85

4.1	TGA and DTG curves of MWCNTs	86
4.2	TGA and DTG curves of MWCNTs-MnO ₂	87
4.3	Raman spectra of a) MWCNTs and b) MWCNTs-MnO ₂	88
4.4	XRD diffractogram of a) MWCNTs and b) MWCNTs-MnO ₂	89
4.5	TEM images of a) MWCNTs and b) MWCNTs-MnO ₂	91
4.6	Polymerization time-temperature profile of PANI polymerized using (NH ₄) ₂ S ₂ O ₈ , K ₂ Cr ₂ O ₇ and KAlSi ₃ O ₈ as oxidizing agents	92
4.7	FTIR spectroscopy of PANI polymerized using a) K ₂ Cr ₂ O ₇ b) KAlSi ₃ O ₈ and c) (NH ₄) ₂ S ₂ O ₈ as oxidant	93
4.8	UV-visible spectra of PANI polymerized using a) K ₂ Cr ₂ O ₇ b) KAlSi ₃ O ₈ and c) (NH ₄) ₂ S ₂ O ₈ as oxidant.	95
4.9	TEM images of PANI oxidized by K ₂ Cr ₂ O ₇	97
4.10	TEM images of PANI oxidized by KAlSi ₃ O ₈	98
4.11	TEM images of PANI oxidized by (NH ₄) ₂ S ₂ O ₈	99
4.12	EDX spectra of a) PANI-K ₂ Cr ₂ O ₇ b) PANI-KAlSi ₃ O ₈ and c) PANI-(NH ₄) ₂ S ₂ O ₈	101
4.13	Uv-visible spectra of a) pristine ex situ PANI/MWCNTs-MnO ₂ and b) PHBSA doped PANI/MWCNTs-MnO ₂	103
4.14	FTIR spectra of a) pristine ex situ PANI/MWCNTs-MnO ₂ and b) PHBSA doped PANI/MWCNTs-MnO ₂	104
4.15	TGA curves of a) pristine ex situ PANI/MWCNTs-MnO ₂ and b) PHBSA doped PANI/MWCNTs-MnO ₂	105
4.16	TEM images of a) pristine ex situ PANI/MWCNTs-MnO ₂ and b) PHBSA doped PANI/MWCNTs-MnO ₂	107
4.17	Proposed interaction between PANI, PHBSA and MWCNTs-MnO ₂	108

4.18	Polymerization time-temperature profiles of PANI, PANI/MWCNTs and PANI/MWCNTs-MnO ₂ .	109
4.19	Proposed mechanism of in-situ polymerization of ES-PANI/MWCNTs-MnO ₂ nanocomposites	111
4.20	FTIR spectroscopy of a) ES-PANI, b) ES-PANI/MWCNTs, c) ES-PANI/MWCNTs-MnO ₂ and d) EB-PANI/MWCNTs-MnO ₂	113
4.21	UV-visible spectra of a) ES-PANI, b) ES-PANI-MWCNTs, c) ES-PANI/MWCNTs-MnO ₂ , d) EB-PANI and e) EB-PANI/MWCNTs-MnO ₂	114
4.22	Raman spectra of a) ES-PANI/MWCNTs-MnO ₂ and b) ES-PANI	115
4.23	XRD diffractogram of a) ES-PANI/MWCNTs-MnO ₂ and b) ES-PANI	117
4.24	TGA curves of a) MWCNTs-MnO ₂ b) ES-PANI c) EB-PANI/MWCNTs-MnO ₂ d) ES-PANI/MWCNTs e) EB-PANI and f) ES-PANI/MWCNTs-MnO ₂ (derivatives shown in insert)	118
4.25	DSC melting curves of a) ES-PANI and b) EB-PANI c) ES-PANI/MWCNTs-MnO ₂ d) ES-PANI/MWCNTs e) EB-PANI/MWCNTs-MnO ₂	119
4.26	a-b) TEM micrograph of unfilled ES-PANI/MWCNT and c) SEM micrograph of unfilled ES-PANI/MWCNT	122
4.27	a-b) TEM micrograph of ES-PANI/MWCNT-MnO ₂ c) SEM micrograph of ES-PANI/MWCNT-MnO ₂	125
4.28	EDX spectrum of ES-PANI/MWCNT-MnO ₂	125
4.29	Polymerization time-temperature profile of ES-PANI/MWCNTs-MnO ₂ at different loading	128
4.30	FTIR spectroscopy of FTIR spectra of a) PANI b) 5% c) 10% d) 20%	129

	e) 30% and f) 50%-ES-PANI/MWCNTs-MnO ₂	
4.31	UV-visible spectra of a) PANI b) 5% c) 10% d) 20% e) 30% and f) 50%-ES-PANI/MWCNTs-MnO ₂ ..	130
4.32	Raman spectra of a) PANI b) 5% c) 10% d) 20% e) 30% and f) 50%-ES-PANI/MWCNTs-MnO ₂ .	132
4.33	XRD diffractogram of a) PANI b) 5% c) 10% d) 20% e) 30% and f) 50%-ES-PANI/MWCNTs-MnO ₂ .	133
4.34	TGA curves of a) PANI b) 5% c) 10% d) 20% e) 30% and f) 50%-ES-PANI/MWCNTs-MnO ₂ .	134
4.35	Conductivity of nanocomposites at different MWCNTs-MnO ₂ loading	135
4.36	Conductivity of ES-PANI/MWCNTs-MnO ₂ and EB-PANI/MWCNTs-MnO ₂ nanocomposites at different MWCNTs-MnO ₂ loading	136
4.37	Conductivity of EB-PANI/MWCNTs-MnO ₂ nanocomposites at low MWCNTs-MnO ₂ loading.	138
4.38	SEM image of a) 0.2wt%-EB-PANI/MWCNTs-MnO ₂ (before percolation) and b) 0.5wt%-EB-PANI/MWCNTs-MnO ₂ (after percolation)	139
4.39	Percolation scaling law between $\log \sigma_c$ and $\log (\Phi - \Phi_c)$	140
4.40	Conductivity of initially doped and redoped ES-PANI/MWCNTs-MnO ₂ nanocomposites at different loading	143
4.41	Proposed interaction of a) ES-PANI/MWCNTs-MnO ₂ in NMP b) EB-PANI/MWCNTs-MnO ₂ in NMP	147

LIST OF PLATES

		Page
4.1	Photograph of MWCNTs-MnO ₂ in a) water-SDS b) water and c) NMP	145
4.2	Photograph of sample suspended in NMP a) green solution of ES-PANI/MWCNTs-MnO ₂ b) green solution of ES-PANI c) blue solution of EB-PANI and d) blue solution of EB-PANI/MWCNTs-MnO ₂	147
4.3	Deposited of the samples on glass substrate a) EB-PANI/MWCNTs-MnO ₂ and b) EB-PANI on glass substrate	148
4.4	After immersion of the deposited samples on glass substrate a) ES-PANI/MWCNTs-MnO ₂ and b) ES-PANI	148

LIST OF ABBREVIATIONS

CNTs	Carbon nanotubes
DSC	Differential scanning calorimeter
EB	Emeraldine base
ES	Emeraldine salt
FTIR	Fourier-transform infrared
HOMO	Highest occupied molecular orbital
LUMO	Lowest unoccupied molecular orbital
MWCNTs	Multiwalled carbon nanotubes
NMP	N-methylpyrrolidinone
PANI	Polyaniline
PEDOT	poly(ethylenedioxythiophene)
PHBSA	Para-hydroxybenzene sulfonic acid
PPy	Polypyrrole
RBM	Radial breathing mode
SDS	Sodium dodecyl sulphate
SEM	Scanning electron microscope
SWCNTs	Singlewalled carbon nanotubes
TEM	Transmission electron microscope
TGA	Thermogravimetric analysis
XRD	X-ray diffraction

LIST OF SYMBOLS

Φ	Volume fraction of the conductive phase
Φ_c	Critical volume fraction
D	Diameter
L	Length
t	Conductivity exponent
ΔH_m	Enthalpy of melting
η	Aspect ratio
σ_c	Effective electrical conductivity of a composite
σ_f	Conductivity of the conductive phase
T_m	Melting temperature

SINTESIS DAN PENCIRIAN KOMPOSITNANO POLIANILIN/TIUBNANO KARBON BERBILANG DINDING

ABSTRAK

Polianilin/tiubnano karbon berbilang dinding -manganese dioksida (PANI/MWCNTs-MnO₂) kompositnano telah disintesis dan diciri. Pengisian MnO₂ telah berjaya dilaksanakan dengan permukaan luar yang bersih melalui mikroskop electron bertransmisi (TEM). Agen pengoksida ammonia persulfat ((NH₄)₂S₂O₈) telah dibuktikan berkesan bagi pembentukan PANI untuk kompositnano. Pengaliran elektrik PANI adalah 38.34 Scm⁻¹ dengan struktur gentian seperti yang dilihat melalui TEM. Kompositnano ex-situ yang baru menunjukkan peningkatan pengaliran elektrik dan interaksi permukaan berbanding kompositnano tanpa asid para-hydroxybenzene sulfonic (PHBSA). TEM menunjukkan peningkatan perlekatan permukaan dengan pengaliran elektrik pada 39.26 Scm⁻¹. Kompositnano PANI/MWCNTs-MnO₂ telah dibuat dengan kaedah in-situ. Pengisian MnO₂ menunjukkan peningkatan dan kesan-kesan yang diperlukan ke atas kompositnano. Kajian struktur dan terma menunjukkan interaksi di antara PANI dan MWCNTs adalah lebih bagus dengan pengisian MnO₂. Pembentukan PANI adalah lebih teratur dan nipis pada permukaan MWCNTs-MnO₂ dengan pengaliran elektrik yang lebih tinggi berbanding kompositnano yang tidak berpengisi. Kompositnano PANI/MWCNTs-MnO₂ pada pengisian yang berbeza menunjukkan pengaliran elektrik meningkat dengan pertambahan MWCNTs-MnO₂. Pengaliran elektrik meningkat ke 78.79 Scm⁻¹ pada 50 wt%. Penilaian pada pengisian MWCNTs-MnO₂ yang rendah menunjukkan kompositnano yang dinyah bendasingkan mengalami penapisan rintangan elektrik pada 0.5 wt% MWCNTs-MnO₂ dan kuasa gandaan pengaliran elektrik, t pada 1.38. Kompositnano PANI/MWCNTs-MnO₂ juga

menunjukkan yang pengaliran elektrik adalah ulang-alik dengan proses meletak dan menyahkan bendasing. Juga dapat diperhatikan bahawa kesan penuaan pengaliran elektrik berkurangan dengan pengisian MWCNTs-MnO₂ pada kompositnano. Kompositnano PANI/MWCNTs-MnO₂ juga menunjukkan pembentukan lapisan yang elok dengan tiada kupasan selepas proses meletak bendasing.

**SYNTHESIS AND CHARACTERIZATION OF
POLYANILINE/MULTIWALLED CARBON NANOTUBES BASED
NANOCOMPOSITES**

ABSTRACT

Polyaniline/multiwalled carbon nanotubes-manganese dioxide (PANI/MWCNTs-MnO₂) nanocomposites were synthesized and characterized. MnO₂ filling in the cavities of the MWCNTs were successfully done with clean outer surface as seen by transmission electron microscope (TEM). Ammonium persulphate ((NH₄)₂S₂O₈) oxidant proved to be desirable for the formation of PANI for the nanocomposite. The electrical conductivity of the polymerized PANI was at 38.34 Scm⁻¹ with a fiber-like structure as observed by TEM. New para-hydroxybenzene sulfonic acid (PHBSA) doped ex-situ nanocomposites exhibit improved electrical conductivity and interfacial interaction compared to the pristine ex-situ nanocomposite without PHBSA. TEM demonstrated clearly the improved bonding at the interface with electrical conductivity up to 39.26 Scm⁻¹. New PANI/MWCNTs-MnO₂ nanocomposites were developed by in-situ method. The MnO₂ filling showed enhanced and desirable effect on the nanocomposite. Structural and thermal studies showed that the interaction between PANI and MWCNTs was more favorable with the addition of MnO₂. The formation of PANI was more uniform and thin on the surface of MWCNTs-MnO₂ with higher electrical conductivity compared to the unfilled nanocomposite. The PANI/MWCNTs-MnO₂ nanocomposites at different loading showed that the electrical conductivity increasing amount of MWCNTs-MnO₂. The electrical conductivity reached up to 78.79 Scm⁻¹ at 50 wt%. Evaluation at low MWCNTs-MnO₂ loading showed that the dedoped nanocomposite exhibit

electrical percolation threshold at 0.5 wt% MWCNTs-MnO₂ and conductivity exponent, t of 1.38. The PANI/MWCNTs-MnO₂ nanocomposites showed that the conductivity was reversible by dedoping and redoping process. It had been observed that the conductivity ageing effect lessened with more amount of MWCNTs-MnO₂ in the nanocomposites. Deposited PANI/MWCNTs-MnO₂ film showed good film formation with no peeling after redoping process.

CHAPTER 1

INTRODUCTION

1.1 Overview

Until about 30 years ago, all polymers were rigidly regarded as insulators. The idea that plastics could be made to conduct electricity would have been considered to be ridiculous. Indeed, plastics have been extensively utilized by the electronics industry for this very property. They are used as inactive packaging and insulating material. The advantages of plastics have always been associated with these typical plastic properties, and those properties included a very low electrical conductivity. For some applications, such as use in electronic packaging and as circuit board material, low conductivity was favorable. This very narrow perspective is rapidly changing as a new class of polymers known as conducting polymers are being discovered. Three scientists have recently shared the Nobel Prize in Chemistry in 2000 for their discovery and development of conductive polymers (Hall, 2003). These three men are: Americans Alan J. Heeger and Alan G. MacDiarmid and Hideki Shirakawa of Japan. The Nobel Prize was awarded because conductive polymers are so different from any other polymeric (plastic) material in their conductivity but are similar to other plastics in their weight, cost, moldability, and general physical properties (MacDiarmid, 1997; Shirakawa, 1997; Heeger, 2001;).

Polyaniline (PANI) is one of the conducting polymers that have a potential near term use due to its good processability, environmental stability, unique conduction mechanism and reversible control of conductivity both by charge-transfer doping and protonation. The susceptibility of PANI to protonation-deprotonation and its controllable changes in electrical conductivity by more than many orders of

magnitude have rekindled intense interest in this polymer. The potential applications of PANI include secondary batteries, supercapacitor materials, electromagnetic interference shielding, nanowires, molecular sensors, nonlinear optical devices, electrochromic displays and microelectronic devices (Dhawan et al., 2003; Sivaraman et al., 2006, Sutar et al., 2007; Ashery et al., 2008; Kalendová et al., 2008; Li et al., 2008; Weng et al., 2009).

Carbon nanotubes (CNTs) have received much interest for their use in fabricating new classes of advanced material due to their unique structural, thermal, mechanical and electronic properties (Yamabe et al., 2001; Astorga and Mendoza, 2005; Qin et al., 2008; Unnikrishnan et al., 2008). The Young's modulus for multiwalled carbon nanotubes (MWCNTs) is higher than single-walled carbon nanotubes (SWCNTs) as determined both experimentally and theoretically (Salvetat et al. 1999). Higher Young's modulus values of MWCNTs compared to SWCNTs are due to the contribution of van de Waals (vdW) force that supports the inner tubes (Meyyappan, 2005).

MWCNTs can be metallic or semiconducting, depending on the crystal structure of the graphene sheets. The electronic transport occurs almost without any electron scattering in the metallic nanotubes. This allows the nanotubes to conduct electricity with minimal resistance, thus diminishing heating (Liang et al. 2001). MWCNTs also behave as like a quantum wire with several orders of magnitude greater in stability than other typical room-temperature quantum conductor due to the confinement effect on the tube circumference (Frank et al., 1998; Liu et al., 2004). The use of MWCNTs as reinforcement in polymers is preferred mainly due to the high vdW forces of which gave higher Young's modulus (Meyyappan, 2005; Coleman et al., 2006).

Transition metals, particularly MnO₂ have shown potentials in improvement of electrochemical, oxidizing and conduction properties of the MWCNTs (Lee et al., 2001; Jiang and Kucernak, 2002; Reddy et al., 2003). MnO₂ is preferred compared to other transition metals due to its good combination of initiator properties (oxidizing the monomer to become polymer) (Gemeay et al. 2008) and conduction properties (flow of electrons) (Wakiya et al. 2001).

MWCNTs/polymer nanocomposites have been pursued with the hope of delivering MWCNT properties to a processable matrix host, with different types of polymer for target applications. MWCNTs have been used as reinforcement or filler in conventional plastics such as polypropylene, poly(vinyl alcohol), epoxy, poly(ethylene oxide) and polycarbonate, (Wanjale and Jog, 2006; Jin et al., 2007; Yang et al., 2009; Abbasi et al., 2010) including rubbers (Das et al., 2008; Lu et al., 2008).

Recently, the uses of conducting PANI together with MWCNTs to form nanocomposites have been reported by several authors (Deng et al., 2002; Sainz et al., 2005; Wu and Lin, 2006; Su et al., 2007). This combination is useful to obtain composites with both the properties of PANI and that of MWCNTs. The application of PANI/MWCNTs composites includes as electromechanical actuation, biosensor applications, gas sensors, supercapacitors, microwave absorption and conducting nanowires (Makeiff and Huber, 2006; Mottaghitlab et al., 2006; Sivakkumar et al., 2007; Wang et al., 2007; Dhand et al., 2008; Srivastava et al., 2009). The use of in-situ technique for the preparation of PANI/MWCNTs offers many advantages to the formation of the nanocomposites over the solution processing (ex-situ) such as high polymerization yield, better interaction and better dispersion of tubes (Deng et al., 2002; Yu et al., 2005; Konyushenko et al., 2006). Ex-situ technique to obtain

PANI/MWCNTs proves to be undesirable (low conductivity, poor dispersion and solvent dependent) (Coleman et al., 2006; Konyushenko et al., 2006).

1.2 Problem statement

Although the studies of in-situ prepared PANI/MWCNTs indicate a unique compatibility between PANI and MWCNTs, the nature of PANI/MWCNTs interaction remains unclear. Furthermore the PANI formation on the unfilled MWCNTs surface is still not uniform and thick regardless of the MWCNTs properties to act as template for polymerization of PANI (Karim et al., 2005; Philip et al., 2005; Konyushenko et al., 2006; Choi et al., 2007; Gopalan et al., 2007; Su et al., 2007). Thin and uniform nanolayer of conducting polymer has been pursued as a way to increase the conductivity by tunnelling mechanism though this is not achievable by using unfilled MWCNTs (Konyushenko et al. 2006). However, the use of MnO₂-filled MWCNTs to generate a ternary PANI based nanocomposite has not yet been investigated. This new material is expected to have enhanced surface interaction and improved properties which may allow tunnelling mechanism.

Electronic conductivity or flow of electron is important for the nanocomposites to be useful for electronic applications. Besides the conductivity, other main important aspects are the doping reversibility (ability of the nanocomposites to achieve initial conductivity values upon changing from insulating to conducting), conductivity ageing (conductivity of the nanocomposites overtime), loading amount of filler (properties of the nanocomposites at different wt% of MWCNTs-MnO₂) and percolation threshold. Few reported the effect of unfilled MWCNTs loading and conductivity ageing on the PANI nanocomposites. Though the nanocomposites properties improved, the use of MnO₂-filled MWCNTs with

PANI is expected to increase the properties even more (Stejskal and Gilbert, 2002; Konyushenko et al., 2006).

Another method of preparing the PANI composites besides the in-situ is the ex-situ method (Coleman et al., 2006; Konyushenko et al., 2006). While this method is a valuable for both MWCNTs de-aggregation and composite formation, its resulting conductivity is usually less (Konyushenko et al. 2006). The compatibility of this method remains a problem because the solvent removal process does not induce any wrapping of tubes usually obtained by in-situ that promotes charge transfer process. In hope to increase the compatibility of PANI with other polymer or solvent using ex-situ method, some authors protonated the PANI by functionalized protonic acids (Heeger, 1992; Cao et al., 1993; Pron et al., 1993; Anitha and Subramanian, 2003; Lee et al., 2009) imparting dopant compatibility with non-polar or weakly polar organic solvents. Though this method is useful for obtaining compatibility with other polymers or solvents, its compatibility with inorganic fillers such as MWCNTs would require another type of dopant with bifunctional characteristic to impart charge instability to the PANI (for conduction) and as well as bridging it with the MWCNTs for charge transfer. Until recently, there is no work has been done on the use of bifunctional dopant (PHBSA) to bridge the PANI and MWCNTs-MnO₂ using ex-situ method. Most of the work only focuses on dopants which can compatibilize PANI with other conventional nonconducting polymers (Paul and Pillai, 2000; Han and Im, 2001, Pud et al., 2003) or solvents (Yin and Ruckenstein, 2000; Hundley et al., 2002) not with inorganic component such as MWCNTs-MnO₂.

1.3 Research objectives

The objectives of this research are:

1. To produce novel in-situ and ex-situ prepared ES-PANI/MWCNTs-MnO₂ nanocomposites with advanced and improved properties.
2. To improve the properties of in-situ ES-PANI/MWCNTs by filling the MWCNTs with MnO₂.
3. To improve the properties of ex-situ prepared ES-PANI/MWCNTs-MnO₂ by using PHBSA as a linking agent and a dopant (bifunctional characteristics).
4. To evaluate the morphology, structural, thermal, interaction between components and electronic conductivity of the ES-PANI/MWCNTs-MnO₂ nanocomposites.

1.4 Scope of study

Introduction of Chapter 1 was discussed with some overview of the research. Chapter 2 will present the literature review of the research with some basic information about nanotechnology, carbon nanotubes, conducting polymers and nanocomposites. Subsequently, literature review was done on various published works, particularly those that are closely related to this work. Chapter 3 discusses the experimental procedures employed in this project. Chapter 4, the results and discussion of the research, focuses on the polymerization study of PANI using several different oxidants, effect of MnO₂ filling on the properties of MWCNTs, properties of the in-situ nanocomposites, ex-situ prepared nanocomposites and the effect of bifunctional linking molecules, effect of different MWCNTs-MnO₂ loading on the properties of the nanocomposites, percolation threshold, reprotonation and conductivity ageing of the nanocomposites and the solubility, color characteristic and

film formation of the nanocomposites. Properties of the nanocomposites will be analyzed by means of data from X-ray diffraction (XRD) to check its crystalline profile, Uv-visible to evaluate the electronic transition, Fourier transform infra red (FTIR) to check the functional group, Raman to check its vibrational properties, Thermogravimetric analysis (TGA) and differential scanning calorimetry (DSC) for thermal stability and transitions, resistivity measurement, scanning electron microscope (SEM) and transmission electron microscope (TEM) for the morphologies and energy dispersive X-ray (EDX) for elemental analysis. Finally, Chapter 5 presents some concluding remarks on the present work as well as some suggestions for further studies.

CHAPTER 2

LITERATURE REVIEW

2.1 Nanotechnology

Nanotechnology is the ability to build or engineer materials, devices and systems with atomic precision, atom by atom. The term nano refers to the length scale of 1 nm or 1×10^{-9} m (Poole and Owens, 2003). There are many reasons why nanotechnology has become so important. The quantum mechanical properties of electrons inside matter are influenced by variations on the nanoscale. By nanoscale design of materials, it is possible to vary their micro and macroscopic properties (Callister, 2003). Developments in nanoscience would allow placing of man-made nanoscale things inside living cells. It would also make it possible to make new materials using the features of nature. Macroscopic systems made up of nanostructures can have much higher density than those made up of microstructure. They can also be better conductors of electricity (Poole and Owens, 2003).

Nanotechnology can be beneficial for human health care, because nanoscience and nanotechnologies have a huge potential to bring benefits in areas as diverse as nanomedicine (Kostoff et al., 2007; Sahoo et al., 2007). Human healthcare nanotechnology research can definitely result in immense health benefits. From nanotechnology, there is a step to nanomedicine, which may be defined as the monitoring, repair, construction, and control of human biological systems at the molecular level, using engineered nanodevices and nanostructures (Whitesides, 2003; Wilkinson, 2003; Jain, 2005). It can also be regarded as another implementation of nanotechnology in the field of medical sciences and diagnostics.

One of the most important issues is the proper distribution of drugs and other therapeutic agents within the patient's body (Jain, 2005).

Probably, the most important application of nanotechnology is the manufacturing of microchips and electronic materials (Poole and Owens, 2003). By reducing the dimensions of the chip components, their number on the chip can be increased, making them even faster because the electric signal has to travel less distance between them (Mamalis, 2007). The dimensions of chip components cannot be reduced in size any further with today's manufacturing methods, because photolithography does not permit the manufacturing of particles with dimensions of 100 nm or less (Mamalis, 2007). By nanotechnology, it is possible to decrease the size of the device (the electronic component and the wires) down to the nanoscopic scale. Single crystals nanowires (diameter: 5–30 nm) have been obtained by chemical vapor deposition using silicon tetrahydride (SiH_4) as starting compound and gold clusters as catalysts. The crystalline silicon core is surrounded by a 1–3 nm thick sheath of amorphous oxide (Cui et al. 2001).

The application of nanotechnology in automobiles ranges from contributions for CO_2 -free engines, safe driving, quiet cars, self-cleaning body and windscreens, up to a self-forming car body (Ahmed et al. 2010). The applications are manifold, from power train, light weight construction, energy conversion, pollution sensing and reduction, interior climate, wear reduction, driving dynamics and surveillance control (Slack et al., 1991; Presting and König, 2003; Ahmed et al., 2010).

In the food industry, several novel applications of nanotechnologies have become apparent, including the use of nanoparticles, such as micelles, liposomes, nanoemulsions, biopolymeric nanoparticles and cubosomes, as well as the development of nanosensors, which are aimed at ensuring food safety (Esposito et

al., 2005; Nasongkla et al., 2006; Yih and Al-Fandi, 2006). Nanoparticles can, for instance, be used as bioactive compounds in functional foods. Bioactive compounds that can be found naturally in certain foods have physiological benefits and might help to reduce the risk of certain diseases, including cancer (Chau et al. 2007).

The potential advantages of nanotechnologies include the opportunities to produce devices that could select and reorganize atoms and molecules with the aim of remedying unbalanced environmental relationships. The possibility of preparing technological products in a ‘‘bottom-up’’ style without producing wasteful and dangerous by-products, as typically occurs with most of today’s current manufacturing processes (Mamalis, 2007) and the ability to produce more functionally efficient materials and devices with higher strength-to-weight ratios (Uskokovic, 2007). Several disadvantages effects of nanotechnology include the potential of nanomaterial to cause harm by reaching target organ in human body by inhalation, ingestion, and dermal penetration (Oberdörster et al. 2005). Unsustainable applications of nanoproducts could further destabilize the already endangered diversity of the ecosystem. Furthermore, the booming nanotechnology based economy could further extend the existing gap between the rich and the poor (Maynard, 2006).

2.1.1 Nanomaterials

Size of nanomaterials ranges from 1 to 100 nm normally in all three dimensions (Poole and Owens, 2003). It was believed that materials with internal structure of nanoscale dimension are hardly new to science. Size of a particle is not the only characteristic of nanoparticles, nanocrystals or nanomaterials. Specific property of many nanomaterials is that the majority of their atoms are located on the surface of a particle as opposed to conventional material, in which atoms are distributed over volume of a particle (Poole and Owens, 2003). Nanomaterials are of great scientific interest as they are effectively a bridge between bulk materials and atomic or molecular structures. A bulk material should have constant physical properties regardless of its size, but at the nano-scale, size-dependent properties are often observed. Thus, the properties of materials change as their size approaches the nanoscale and as the percentage of atoms at the surface of a material becomes significant (Kruis and Josh, 2005). For bulk materials larger than one micrometer, the percentage of atoms at the surface is insignificant in relation to the number of atoms in the bulk of the material (Mark and Horenstein, 2009). The interesting and sometimes unexpected properties of nanomaterials are therefore largely due to the large surface area of the material, which dominates the contributions made by the small bulk of the material (Mark and Horenstein, 2009).

Sheet silicates (phyllosilicates) are examples of natural nanomaterials used in nanotechnology (Pavlidou and Papaspyrides, 2008). The crystal lattice of 2:1 layered silicates, consists of two-dimensional layers where a central octahedral sheet of alumina is fused to two external silica tetrahedra by the tip, so that the oxygen ions of the octahedral sheet also belong to the tetrahedral sheets (Pavlidou and Papaspyrides, 2008). The layer thickness is around 1 nm and the lateral dimensions may vary from

300Å to several microns, and even larger, depending on the particulate silicate, the source of the clay and the method of preparation. Therefore, the aspect ratio of these layers (ratio length/thickness) is particularly high, with values greater than 1000 (Beyer, 2002; McNally et al., 2003). Zeolites (aluminosilicates) are another example of natural occurring nanomaterials. The crystalline structure of zeolites is formed by tetrahedral molecular fragments of silica and alumina. These structure formed cavities and channels that contain water molecules and metal cations, its rarely pure and are contaminated to varying degrees by other minerals, metals, quartz, or other zeolites. For this reason, naturally occurring zeolites are excluded from many important commercial applications where uniformity and purity are essential (Zoe et al., 2005). Naturally occurring zeolites forms are of limited value, because they almost always contain undesired impurity phases and their chemical composition varies from one deposit to another (Weitkamp, 2000). Zeolites have been found to be very effective at removing ammonia from water due to their excellent ion exchange capacity (Lei et al., 2009).

Copper nanoparticles in different stoichiometries are semiconductors with p-type conductivity, and have been widely used in optical filters and superionic materials. The thermal stability and the band gaps of copper nanoparticles vary depending on their stoichiometries or phases (Wang et al., 1998; Nasibulin et al., 2000; Seoudi et al., 2007; Schwarz et al., 2009). The composition and the crystal structure of the final products are usually dependent on the preparation methods (Seoudi et al. 2007). Copper nanoparticles smaller than 50 nm, are considered super hard materials that do not exhibit the same malleability (easily to be formed) and ductility as bulk copper (Dubbs and Aksay, 2000). Another interesting type of nanomaterial is gold nanoparticles. One of the most promising applications of gold

nanoparticles is in colorimetric sensors for specific target detection. Aggregation of gold nanoparticles leads to a change in their optical properties (a red shift in surface plasmons, or a red to blue color change), which can be used in the colorimetric detection of target agents (Kim et al., 2008). Thin gold nanoparticles have been used to coat iron. The gold shell on the surface has proved effective at preventing oxidation of the iron (Carpenter et al., 2000). Silica is an abundant compound over the earth largely employed in industries to produce silica gels, colloidal silica and fumed silica (Barik et al. 2008). The nanosized silicas are interesting particles because they are applied in emerging areas like medicine and drug delivery (Barik et al. 2008). Silica nanoparticles have been used in the industry to reinforce the elastomers as a rheological solute (Chrissafis et al. 2008).

2.1.2 Properties and applications carbon nanotubes (CNTs) and other allotropes of carbon

In order to understand the structure and properties of CNT, the bonding and the properties of carbon atoms will be discussed. Carbon is an element that exists in various polymorphic or allotropic forms. Although the element is essentially carbon, it can exist in several kinds of structures and forms such as graphite, diamond, fullerene and CNT that contributes significantly to the different behaviour from each other (Gogotsi, 2006).

In graphite as in Figure 2.1 (Callister, 2003), the outer shell electrons of each carbon atom occupy the planar sp^2 hybrid orbital forming an in plane σ bond with other carbon atoms and an out plane π orbital which is further delocalized (Callister, 2003). This type of covalent bonding forms a hexagonal network layer of carbon atoms. These layers are parallel with each other and held by van der Waals (vdW)

force. The weak vdW interaction makes graphite easily slip along the plane axis. The loose π electrons are distributed along the plane axis hence making graphite electrically conductive along that axis (Callister, 2003). The resistivity value of graphite reached up to $7.837 \mu\Omega\text{m}$ (Steiner, 2010). The electrical conductivity of composites obtained by mixing epoxy resin and graphite have shown that the conductivity changes of up to 11 orders of magnitude were observed as the filler load increased from 0 to 8 wt%, while the percolation threshold was around 3 wt% (Jović et al. 2008). In-situ polymerization of styrene to form polystyrene in the presence of graphite has shown that the conductivities of the composites increase as the number of ordered graphite layers increases. The electrical conductivity reached up to $1.3 \times 10^{-1} \text{ Scm}^{-1}$ with 10 wt% graphite loading (Kim et al. 2007).

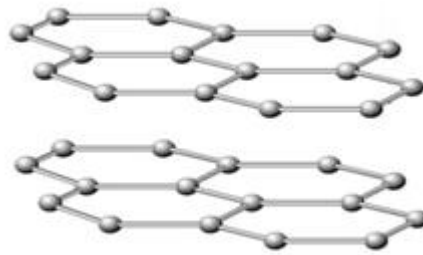


Figure 2.1 Physical structure of graphite (Callister, 2003).

Another polymorph of carbon is diamond as seen in Figure 2.2 (Callister, 2003). Diamond has a zinc blend structure, where each carbon atom bonds covalently to four other carbon atoms. All the valence electrons of each carbon occupy sp^3 hybrid orbital thus forming a tetrahedral bond with the other carbon atoms (Callister, 2003). Unlike graphite, diamond has an interlocking network structure consisting of only σ bonds without any delocalized π electrons. The electrons within the σ bonds are tightly held. This makes diamond the hardest known

material which is electrically insulating with high thermal conductivity. Diamond has high electrical resistivity: 10^{11} to $10^{18} \Omega\text{m}$ (Pierson, 2004). The conductivity of Iodine doping on diamond film deposited on Si substrate were found to be increased from 8.26×10^{-4} to $2.76 \times 10^{-2} \text{Scm}^{-1}$ (Omer et al. 2006).

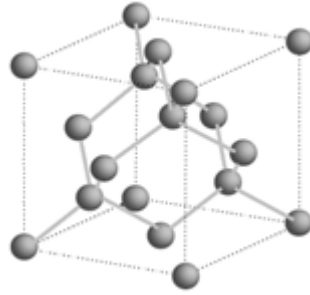


Figure 2.2 Physical structure of diamond (Callister, 2003).

The market for industrial-grade diamonds operates much differently from its gem-grade counterpart. Industrial diamonds are valued mostly for their hardness and heat conductivity, making many of the gemological characteristics of diamonds, such as clarity and color, irrelevant for most applications (Pace et al. 2000). Industrial use of diamonds has been associated with their hardness (Tönshoff et al. 2000); this property makes diamond the ideal material for cutting and grinding tools. As the hardest known naturally occurring material, diamond can be used to polish, cut, or wear away any material, including other diamonds. Common industrial adaptations of this ability include diamond-tipped drill bits and saws, and the use of diamond powder as an abrasive (Tönshoff et al. 2000). The term nanodiamond is used for diamond-based materials at the nanoscale, including pure phase diamond films, diamond particles, and their structural assemblies, such as loosely bound particle agglomerate or particles incorporated into other material matrices (Barnard, 2006). It is possible to synthesize nanodiamonds with narrow size distribution using the

methods of detonation, CVD and energetic beam implantation in laboratories (Praver et al., 2000; Barnard, 2006). Nanodiamond films have been suggested as an ideal platform for future biochips and biosensors because of their superior properties compared to glass, silicon and gold surfaces (Puzyr et al., 2004).

Fullerenes (C_{60}) are considered as having a closed-shell configuration consisting of 60 carbon atoms forming 20 hexagons and 12 pentagons as seen in Figure 2.3 (Callister, 2003). The bonding is sp^2 mixed with sp^3 due to its high curvature. In its solid state, this spherical molecule forms a crystalline structure of face centered cubic (FCC) with each of the fullerenes occupying the FCC lattice (Callister, 2003). The characteristic reaction of fullerenes is electrophilic addition at 6,6-double bonds, which reduces angle strain by changing sp^2 -hybridized carbons into sp^3 -hybridized ones. The change in hybridized orbital causes the bond angles to decrease from about 120 degrees in the sp^2 orbitals to about 109.5 degrees in the sp^3 orbitals. This decrease in bond angles allows for the bonds to bend less when closing the sphere or tube, and thus, the molecule becomes more stable (Kratschmer et al., 1990; Parker et al., 1992; Ishida et al., 2001; Cousseau et al., 2006; Zeynalov et al., 2009). Fullerenes are sparingly disperseable in many solvents. Common solvents for the fullerenes include aromatics, such as toluene, and others like carbon disulfide (Wang et al. 2001). Fullerenes hold great promise in health and personal care applications where prevention of oxidative cell damage or death is desirable, as well as in non-physiological applications where oxidation and radical processes are destructive (Zeynalov et al. 2009). Fullerenes chemically reactive and can be added to polymer structures to create new copolymers with specific physical and mechanical properties. They can also be added to make composites. Much work has been done on the use of fullerenes as polymer additives to modify physical properties

and performance characteristics (Wang et al., 2004; Tasaki et al., 2007). Fullerene can be used as organic photovoltaics. The fullerene acts as the n-type semiconductor (electron acceptor). The n-type is used in conjunction with a p-type polymer (electron donor), typically a polythiophene. They are blended and cast as the active layer to create what is known as a bulk heterojunction (Kim et al., 2001; Segura et al., 2005). A study done on poly [2-methoxy-5-(2'-ethyl) hexoxy-1,4-phenylenevinylene] and fullerene composite have shown that the composites conductivity increased by four orders of magnitude as the fullerenes concentration increases to 40 vol%. The conductivity was measured to be about $3 \times 10^{-2} \text{ Sm}^{-1}$ at 65 vol% (Ltaief et al. 2004). A comparative study on ES-PANI–fullerene composites was done by solid-state blending of components and by the introduction of fullerene during polymerization of aniline (in-situ). Composite prepared by solid-state blending had a lower conductivity ($1.5 \times 10^{-7} \text{ Scm}^{-1}$) than the in-situ composite ($7.2 \times 10^{-5} \text{ Scm}^{-1}$). It was suggested that the mechanical blending of the components leads to a decrease in the size of fullerene crystallites. In the in-situ composite, the formation of a PANI–fullerene complex comprising the structure corresponding to a doped polyaniline was observed (Sapurina et al. 2000).

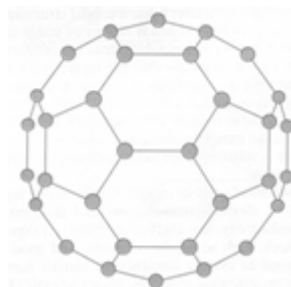


Figure 2.3 Physical structure of fullerene (Callister, 2003).

Recently identified carbon polymorph is the highly interesting CNTs. There are two main types of CNTs; singlewalled carbon nanotubes (SWCNT) and multiwalled carbon nanotubes (MWCNT). The structure of SWCNT can be considered as a single sheet of graphite being rolled into tubes with closed ends made out of fullerene as shown in Figure 2.4 (Callister, 2003). A SWCNT can be envisioned as a narrow rectangular strip of nanoscale graphene with carbon atoms, rolled up into seamless cylinder 1-10 nm in diameter (Callister, 2003). Whereby graphene refers to a monolayer of sp^2 bonded carbon atoms. SWCNTs and also MWCNTs may be classified into three different types: armchair, zigzag and chiral nanotubes, depending on how the two-dimensional graphene sheet is "rolled up". If integers n and m are the number of unit vectors of a graphene structure, the different types of CNTs can be characterized by using these integers (Meyyappan, 2005). Figure 2.5 (Odom et al., 2001) illustrates the 'zigzag' ($n, 0$), 'armchair' (n,n) and 'chiral' (n,m) structures of CNTs. The conductivity of an individual CNTs (n,m) depends on the helical orientation of the hexagonal rings in the walls of the nanotube i.e. on the n and m in a following way. CNTs is metallic when $2n + m = 3q$ with q being an integer and CNTs is a semiconductor when $2n + m \neq 3q$ (Saito et al., 1992).

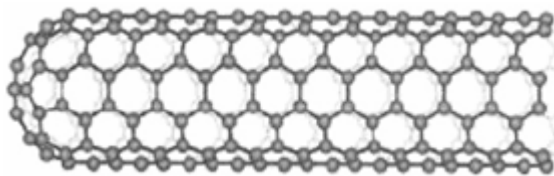


Figure 2.4 Physical structure of SWCNT (Callister, 2003).

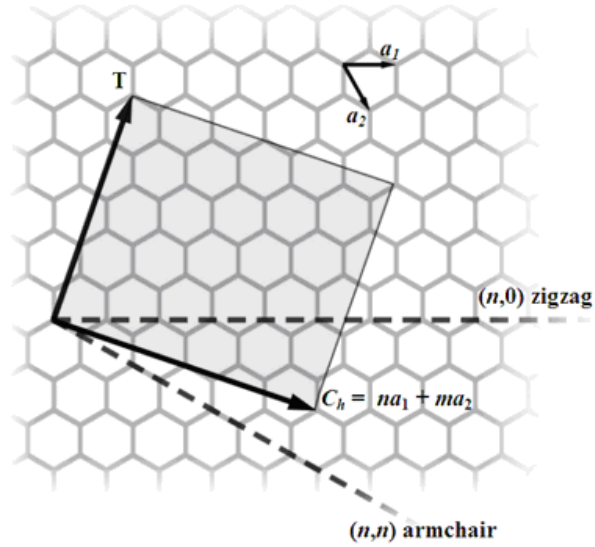


Figure 2.5 Rolling up graphene sheet to form zigzag, armchair and chiral SWCNT/MWCNT (Odom et al., 2001).

It is suggested that a SWCNT should be at least 0.4 nm large to afford strain energy and at most 3 nm large to maintain tubular structure and prevent collapsing. Larger SWCNTs tends to collapse unless it is supported by other forces or surrounded by neighbouring tubes (Meyyappan, 2005). SWCNTs are usually obtained in the form of so-called ropes or bundles, containing between 20 and 100 individual tubes packed in a hexagonal array (Khatri et al., 2009). As reported by Du et al., (2006), CO₂ assisted electrical arc approach is able to produce SWCNTs with controlled length and bundle size. Studied by Huang et al., (2002), after removal of most of the impurities and water, macroscopic and well-aligned SWCNTs bundles up to several centimeters long are formed in a rotary evaporator. Rope formation is energetically favourable due to the vdW attractions between isolated nanotubes (Cao et al., 2007). Also showed by Golberg et al., (2000), SWCNTs typically crystallize in bundles or ropes due to attraction to each other from vdW forces. SWCNTs were prepared by suspending between metal contacts bilayers. The SWCNTs are assembled in ropes of a few hundred parallel tubes (Kasumov et al., 2003).

The rolling up of graphene sheet to form MWCNTs are the same as SWCNT as shown in Figure 2.5 but with multi layers of graphene sheet stacked up together (Meyyappan, 2005). MWCNTs consist of an array of graphite layers forming concentric tubes as presented in Figure 2.6 (Callister, 2003). The tubes are held together by vdW forces. The inner hollow core is often quite large with a diameter commonly about half of that of the whole tube (Meyyappan, 2005). The graphite sheet may be rolled in different orientations along any two-dimensional lattice vector (m,n) which then maps onto the circumference of the resulting cylinder; the orientation of the graphite lattice relative to the axis defines the chirality or helicity of the nanotube. When a graphite sheet is rolled to form a nanotube, the sp^2 hybrid orbital is deformed for rehybridization of sp^2 toward sp^3 orbital or σ - π bond mixing. This rehybridization and π electron confinement contributes to its extraordinary electronic, mechanical, chemical, thermal, magnetic and optical properties (Salvetat and Rubio, 2002; Yokoi et al., 2005; Deng et al., 2009; Xia et al., 2009).

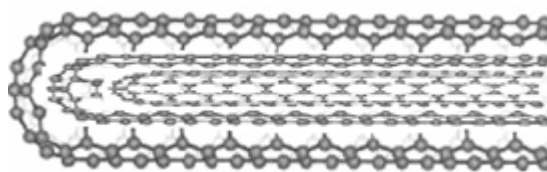


Figure 2.6 Physical structure of MWCNT (Callister, 2003).

The strength of the C-C bond gives rise to interest in the mechanical properties of CNTs. Theoretically; they are stiffer and stronger than any known substance. σ bonding is the strongest in nature, and thus nanotube that is structured with all σ bonding is regarded as the ultimate fiber with the strength in its tube axis (Salvetat and Rubio, 2002). In general, defect free nanotubes are stronger than graphite. This is mainly because the axial component of σ bonding is greatly increased when a graphite sheet is rolled over to form a cylindrical structure. Young's modulus is independent of tube chirality, but dependent on tube diameter. Large tube is approaching graphite and smaller one is less mechanically stable (Gogotsi, 2006; Cao et al., 2007). The Young's modulus for MWCNTs is higher than SWCNTs, typically 1.1 to 1.3 TPa, as determined both experimentally and theoretically (Kuang and He, 2009). Higher Young's modulus values of MWCNTs compared to SWCNTs are due to the contribution of vdW force that supports the inner tubes (Meyyappan, 2005). TEM-based pulling and bending tests gave modulus and strength of MWCNT of 0.8 and 150 GPa, respectively (Gogotsi, 2006). On the other hand, when many SWCNTs are held together in a bundle or rope, the weak vdW force induces a strong shearing among the packed SWCNTs (Cao et al. 2007).

Simulations demonstrate a remarkable “bend, don't break” response of individual SWCNT to large transverse deformation shown in Figure 2.7a (Ijima et al. 1996). The two segments on either side of the buckled region can be bent into an acute angle without breaking bonds with full recovery of a straight perfect tube once the force is removed (Ijima et al., 1996). Similar behaviour has been simulated when the tube is stressed under torsion angle of 60 degrees as in Figure 2.7b (Yu et al. 2004). This fantastic property of mechanical strength allows for these structures to be

used as possible reinforcing materials. These nanotube reinforcers would allow for very strong and light materials to be produced.



Figure 2.7 Molecular dynamics simulation of a) single kink of bending of a SWCNT (Ijima et al., 1996). b) under torsion of a SWCNT (Yu et al., 2004).

It can be expected that CNTs have similar thermal properties to that of graphite and diamond at room and elevated temperatures but unusual behaviour at low temperatures because of the effects of phonon quantization (Gogotsi, 2006). Thermal conductivity of individual MWCNTs has been measured to be more than 3000 W/mK at room temperature (Kim et al. 2001). This high thermal conductivity have potentials to be used as thermal management applications, either as heat pipes in microelectronic packaging and or as alternatives to metallic particle fillers (Zhang et al. 2007). Array of vertically aligned CNTs grown using plasma enhanced chemical vapor deposition exhibits good thermal properties that is ideal for chip cooling as shown in Figure 2.8 (Xu and Fisher, 2006). Recent research has discovered the use of CNTs and carbon nanofibers as fillers for thermal interface material (Biercuk et al., 2002; Cola et al., 2009).

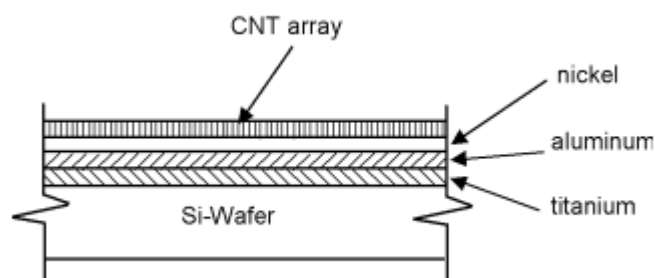


Figure 2.8 Sketch of the CNT array on a silicon wafer (Xu and Fisher, 2006).

Electronic properties of CNTs have received greatest attention because of its small size and highly symmetric structure which allow for remarkable quantum effects. In terms of its conductivity, CNTs can be regarded as semiconducting or metallic (Gogotsi, 2006). The resistivity of MWCNTs is found to decrease with temperature values up to $0.4 \mu\Omega\text{m}$ (Hongjie et al., 1996), while a study on MWCNTs bundle at temperatures between 300 and 1900 K have shown that the resistivity decreases with increasing temperatures (Barberio et al., 2007). The π electrons are more delocalized in CNTs because of σ - π rehybridization and thus give rise to higher conductivity than that of graphite. MWCNTs also behave as like a quantum wire with several orders of magnitude greater in stability than other typical room-temperature quantum conductor due to the confinement effect on the tube circumference (Frank et al., 1998; Liu et al., 2004). The conductivity of transparent films made from SWCNTs was estimated in terms of the average bundle diameter in the SWCNTs films, revealing that there is an increase in film conductivity as the average bundle diameter decreases (Shin et al. 2009). It is found that the adsorption of some gas molecules can cause a change in the electrical conductivity of metallic CNTs of both zigzag and armchair (Mousavi, 2010). Another study has shown that the electrical properties of CNTs are influenced by electron beam irradiation. The

contact resistance decreases by orders of magnitude when exposed to electron beam (Gupta et al. 2007).

CNTs have been used as templates for producing nanowires by combination of metal overcoat. This CNT based nanowires are important for electronic miniaturization (Banerjee et al. 2005). Due to its outstanding conduction properties, CNTs are suggested as an interconnect material for fabrication of microchips (Kreupl et al., 2002, Yung et al., 2009), shown in Figure 2.9 (Xu and Fisher, 2006). The comparison of CNT interconnect with gold-nanowires shows that they can keep up with ordinary metallization schemes at reduced dimensions and can provide a solution for even more demanding requirements on current densities and endurance (Kreupl et al. 2002). Recently, a study report a high-performance fully transparent conducting thin-film transistors on both rigid and flexible substrates with transfer printed aligned nanotubes as the active channel and indium-tin oxide as the source, drain, and gate electrodes. Such transistors have been fabricated through low-temperature processing, which allowed device fabrication even on flexible substrates. The image is shown in Figure 2.10 (Ishikawa et al. 2009). CNTs have been shown to have excellent emission characteristic. CNT emitters can be fabricated in a variety of configurations depending on the nature of the CNTs, microscopic arrangement, preparation process and desired emitter structure. This emission characteristic has wide applications such as field emission displays, microwave amplifiers and vacuum microelectronics (Saito et al., 2000; Liu et al., 2004; Wang et al., 2006).



Figure 2.9 A single MWCNT interconnect (Xu and Fisher, 2006).

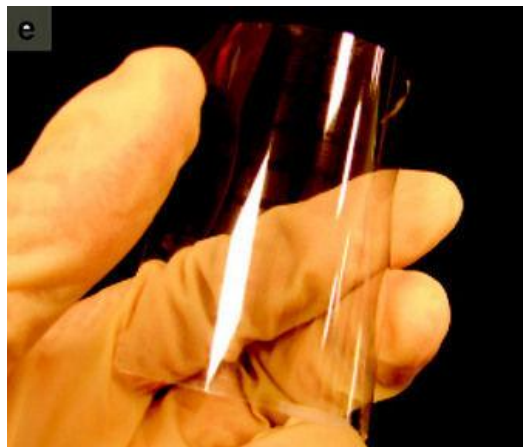


Figure 2.10 Transparent thin-film transistors of CNTs (Ishikawa et al. 2009).